A Global Cloud Database from VIRS and MODIS for CERES

Patrick Minnis, David F. Young, Bruce A. Wielicki
Atmospheric Sciences, NASA Langley Research Center, Hampton, VA USA

Sunny Sun-Mack, Qing Z. Trepte, Yan Chen
SAIC, Hampton, VA USA

Patrick Heck
AS&M, Inc., Hampton, VA USA

Xiquan Dong
University of North Dakota, Grand Forks, ND, USA

Extended Abstract for
SPIE 3rd International Asia-Pacific Environmental Remote Sensing Symposium 2002: Remote Sensing of the Atmosphere, Ocean, Environment, and Space
Hangzhou, China
October 23-27, 2002

A Global Cloud Database from VIRS and MODIS for CERES

Patrick Minnis*[a], David Young[a], Bruce A. Wielicki[a], Sunny Sun-Mack[b], Qing Z. Trepte[b]
Yan Chen[b], Patrick W. Heck[c], Xiquan Dong[d]

[a]Atmospheric Sciences, NASA Langley Research Center, Hampton, VA USA; [b]SAIC, Hampton, VA USA; [c]AS&M, Inc., Hampton, VA USA; [d]Dept. of Atmospheric Sciences, University of North Dakota, Grand Forks, ND USA

ABSTRACT

The NASA Clouds and Earth's Radiant Energy System (CERES) Project has developed a combined radiation and cloud property dataset using the CERES scanners and matched spectral data from high-resolution imagers, the Visible Infrared Scanner (VIRS) on the Tropical Rainfall Measuring Mission (*TRMM*) satellite and the Moderate Resolution Imaging Spectroradiometer (MODIS) on *Terra* and *Aqua*. The MODIS data are taken globally at least twice per day at two local times while the VIRS data are taken at all times of day over a 46-day precession cycle between 37°N and 37°S. Thus, the diurnal cycle can be well-characterized over most of the globe using the combinations of *TRMM*, *Aqua*, and *Terra* data. The cloud properties are derived from the imagers using state-of-the-art methods and include cloud fraction, height, optical depth, phase, effective particle size, emissivity, and ice or liquid water path. These cloud products are convolved into the matching CERES fields of view using the scanner point spread functions to provide simultaneous cloud and radiation data at an unprecedented accuracy. Results are available for at least 3 years of VIRS data and 1 year of *Terra* MODIS data. The various cloud products are compared with similar quantities from climatological sources and instantaneous active remote sensors. The cloud amounts are very similar to those from surface observer climatologies and are 6-7% less than those from a satellite-based climatology. Optical depths are 2-3 times smaller than those from the satellite climatology, but are within 5% of those from the surface remote sensing. Cloud droplet sizes and liquid water paths are within 10% of the surface results on average for stratus clouds. The VIRS and MODIS retrievals are very consistent with differences that usually can be explained by sampling, calibration, or resolution differences. The results should be extremely valuable for model validation and improvement and for improving our understanding of the relationship between clouds and the radiation budget.

radiation, clouds, remote sensing, cloud microphysics, climatology, MODIS, CERES, VIRS

1. INTRODUCTION

Cloud optical and physical properties are essential for linking the hydrological cycle with the Earth's radiation budget (ERB). Simultaneous measurements of cloud properties and broadband radiative fluxes provide the empirical basis for accurate modeling of both processes in climate models. The Clouds and Earth's Radiant Energy System (CERES) project is designed to provide such measurements by matching very consistent cloud properties with radiation budget data for several different satellites [1]. CERES is currently using three multispectral imagers, the Visible Infrared Scanner (VIRS) on the Tropical Rainfall Measuring Mission (*TRMM*) satellite and the Moderate Resolution Imaging Spectroradiometer (MODIS) on *Terra* and *Aqua*, to remotely sense a wide range of cloud properties on a global basis at different times of day coincident with the CERES broadband flux data. These cloud properties have already been used to develop a host of new models that characterize the anisotropy of the radiation field exiting the Earth leading to improved estimates of the ERB from radiance measurements like those from CERES [2, 3]. They will also be valuable for relating the hydrological cycle and the ERB and for improving climate model processes. This paper presents the results from the analysis of VIRS data and compares the VIRS and initial MODIS results to determine the consistency of the cloud products.

*Corresponding author address: P. Minnis, MS 420 NASA Langley Research Center, Hampton, VA 23681
Email address: p.minnis@larc.nasa.gov

2. DATA & METHODOLOGY

The *TRMM*, launched during late 1997, continues to provide coverage at all local hours between 37°N and 37°S over a 46-day period, while *Terra*, operating since Spring 2000, has a 1030 LT equatorial crossing providing twice-per-day coverage in the Tropics and midlatitudes and higher temporal sampling in polar regions. *Aqua* has a 1330 LT equatorial crossing and began producing MODIS imagery in early summer 2002. Except for the 1.6-μm channel gain, which appears to be degrading, the VIRS calibrations were steady during the first 4 years of operation [4, 5]. The *Terra* MODIS thermal-channel brightness temperatures were all within $\pm$ 0.7 K of their VIRS counterparts and the MODIS VIS reflectance was 3% greater (less) than the corresponding VIRS reflectance at the high (low) end of the range. Every other 1-km MODIS pixel and scan line was skipped to achieve an effective 2-km resolution to minimize processing time and data storage.

Each MODIS and 2-km VIRS pixel is initially classified as clear or cloudy using updated versions of the CERES classification schemes [6, 7] that rely on the radiances taken at 0.64 (visible), 1.6 (near infrared), 3.7 (solar infrared), 11 (infrared), and 12 (split window) μm. The radiances are compared with predicted clear-sky radiances based on empirical estimates of spectral clear-sky albedo [8, 9] and on skin temperatures from the European Center for Medium-range Weather Forecasting (ECMWF) reanalyses adjusted using empirical estimates of spectral surface emissivity [10, 11] and atmospheric absorption calculated with the ECMWF vertical profiles of temperature and humidity. Cloud temperature T_c, height z_c, thickness, phase, effective droplet radius r_e or effective ice crystal diameter D_e, optical depth τ, and water path *WP* are derived from these same radiances using one of three methods. The visible infrared solar-infrared split-window technique (VISST), an updated version of the 3-channel daytime method [12], is used during daytime, defined as the time when the solar zenith angle *SZA* is less than 82°. At night, the solar-infrared infrared split-window technique (SIST) is used to determine all of the parameters. The SIST, an improved version of the 3-channel nighttime method [12], uses thermal infrared data only. Thus, its retrievals are valid only for optically thin clouds. For clouds with $\tau < 8$ at night, default values are used for all parameters except phase, T_c, and z_c. The third method [13], the solar-infrared infrared near-infrared technique (SINT) is only applied to MODIS data during the daytime for clouds over snow or ice backgrounds. The determination of the background surface as snow or ice can either come from the scene classification for adjacent clear pixels or from the snow and ice maps used in the CERES data stream [8, 9]. All of the methods compute ice and liquid water solutions that simultaneously determine T_c, τ, and particle size by matching the observed radiances to emittance and reflectance parameterizations that account for atmospheric attenuation and surface reflectance and emission. The cloud reflectances and emittances are included in the parameterizations using updated lookup tables for each specific channel [14]. The phase is selected for each pixel based on the cloud temperatures, the availability of a solution, and the altitude of the cloud.

The pixel-level data are convolved into the footprint (10-20 km) of each CERES radiance to provide the link between clouds and the radiation budget. These single-scanner footprint (SSF) products include the cloud fraction and mean associated properties for up to two cloud layers. Edition-2 VIRS cloud products, currently available for January 1998 - August 2001, will be processed as long as the VIRS data are available. CERES Edition-1 MODIS cloud properties have been completed for December 2000 and 1 – 16 June 2001 (no MODIS data for the remainder of June 2001). Analysis of the *Terra* MODIS data is proceeding to provide a continuous long-term record, while preliminary analysis of the *Aqua* MODIS data has just begun.

3. VALIDATION

A variety of methods are being used to verify the results including climatology, surface data, and other satellite observations. The mean zonal cloud amounts from MODIS for June 2001 and from surface observations taken between 1971 and 1996 [15] in Fig. 1a generally agree well in magnitude and distribution. Exceptions include Antarctica where

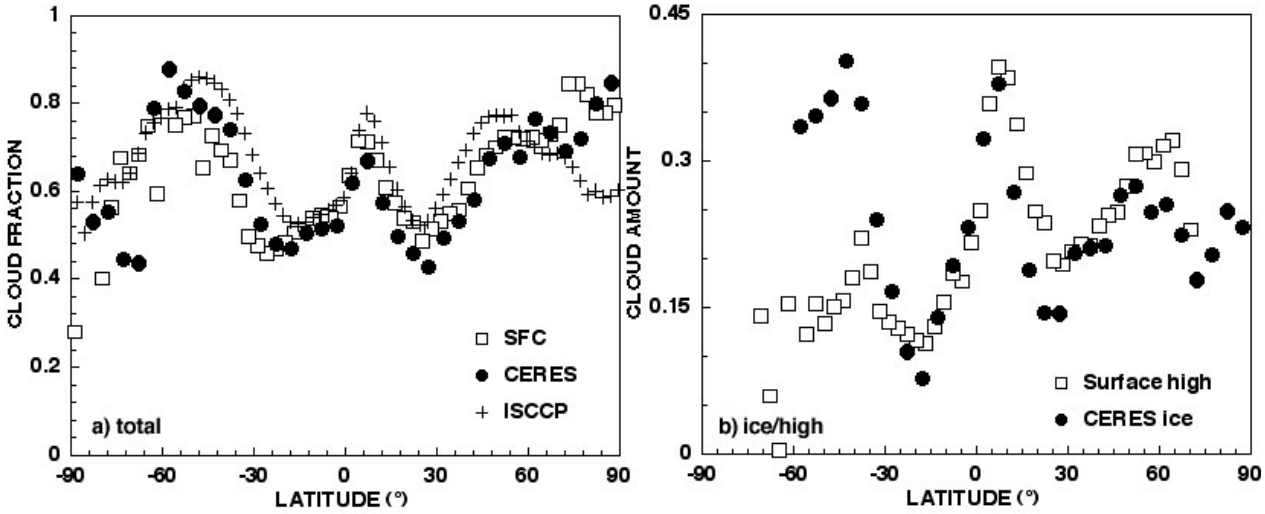

Fig. 1. Mean June total and high/ice cloud fraction from surface (1971-96), ISCCP (1984-91), CERES MODIS (2001).

the surface observations report less cloud cover on average, the southern oceans, and around 75°N. All of these areas are sparsely sampled in the surface dataset relative to the other zones. The results in Fig. 1a are similar to those for December 2000 and to the comparisons using VIRS and surface data [16], except that the retrieved cloud fraction in the Arctic during December 2000 is considerably smaller than the surface climatology, perhaps to due to some errors in the CERES polar mask. The CERES MODIS-derived mean cloud amounts follow the same trends, but are typically 7-8% less than those from the 1984-1991 International Satellite Cloud Climatology Project (ISCCP) D2 dataset [17]. The smaller cloud amounts from CERES may be due to several factors including the use of higher resolution pixels (1-km compared to 8-km ISCCP pixels) and a variety of viewing zenith angles compared to the fixed values for ISCCP. The surface observations report cloud top, but not phase. The closest comparable dataset for phase comparison would be for high clouds (cirrus and cumulonimbus) as observed from the surface. Such cloud reports will not include all of the high clouds in high latitudes where the tops of the clouds may be ice or the midlevel altostratus clouds mat also be ice. The CERES ice cloud amounts are very close to the high cloud amounts in Fig. 1b between 30°S and 10°N and between 30°N and 50°N, but exceed the high cloud amounts south of 30°S and are less than the surface-based high cloud amounts elsewhere. Although the initial results from both visual examination of the images and the zonal mean comparisons indicate that the CERES phase fractions are reasonable, additional analyses are needed to confirm the overall phase determination accuracy.

The CERES-derived cloud optical depths are also substantially greater than those determined from the ISCCP (Fig. 2). During both December 2000 and June 2001, the CERES mean cloud optical depths are 2 to 3 times larger than those from ISCCP, except over the polar regions. Because CERES uses the SINT in those areas, the cloud optical depths are generally much smaller than those that would have been derived using the visible channel for optical depth retrieval. The ISCCP does not have the combination of 1.6 and 3.7-μm channels that is necessary for applying the SINT. Part of the reason for larger optical depths for CERES in non-polar regions is the smaller cloud fraction. Other sources of the discrepancy may be differences in the absolute calibrations used for the various ISCCP satellites and MODIS and temporal sampling. These differences will need further examination to fully determine their cause.

Combinations of active and passive remote sensing of clouds at the surface are extremely valuable for obtaining objective and a more absolute assessment of the derived cloud properties than is possible using surface and satellite climatologies. The approach used to compare cloud properties derived from surface radar and radiometer data to similar quantities derived from geostationary satellite radiances [18] has been employed to verify the derived cloud properties over the Atmospheric Radiation Measurement (ARM) Southern Great Plains (SGP) site near Lamont, Oklahoma. Cloud boundaries were determined using a combination of ceilometer, lidar, and radar data, while cloud properties were retrieved using a combination of radar and microwave and shortwave radiometer data [19]. Surface-derived cloud properties averaged for an hour centered on the satellite overpass time are compared to 30-km x 30-km mean values of the same parameters derived with the CERES algorithm. Figure 3 compares the effective cloud heights for optically thin

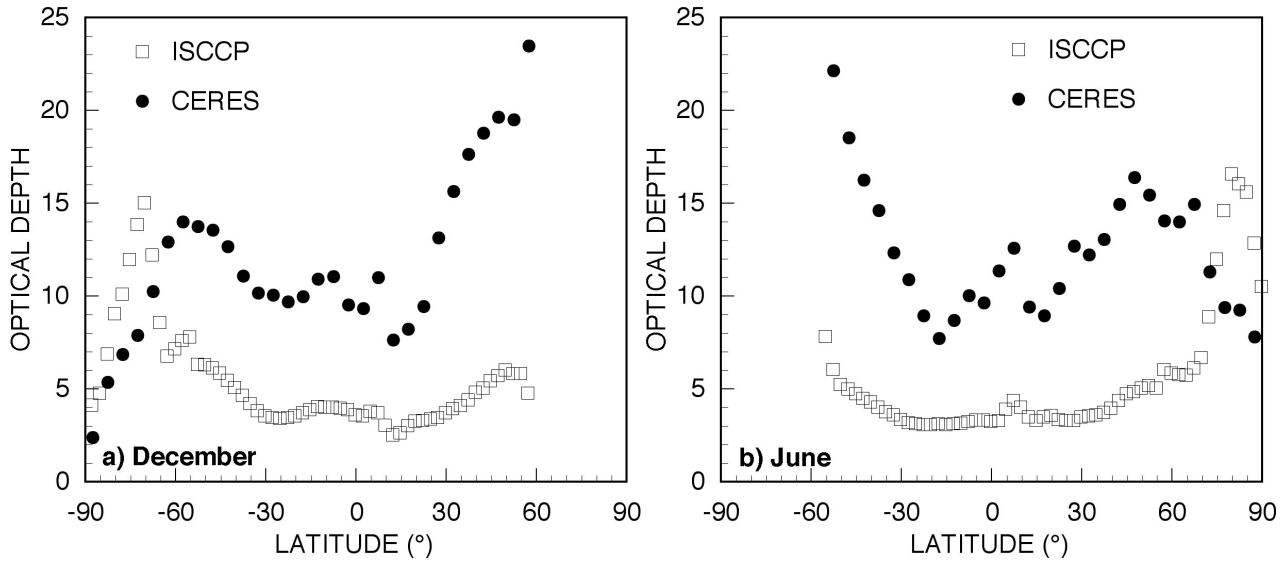

Fig. 2. Mean zonal cloud optical depth from CERES MODIS (December 2000, June 2001) and ISCCP (1984-91).

clouds (τ < 5). CERES converts the derived effective cloud radiating temperature T_c to z_c using the ECMWF temperature profiles. The radiating temperature should correspond to some altitude between cloud base and cloud top. For optically thin clouds, the z_c should be close to the center of the cloud. As the cloud thickens, z_c should become closer to the top of the cloud, assuming the particle density of the cloud increasing. In Fig. 3a, during the daytime, z_c is 0.4 km below the center of the cloud, while at night (Fig. 3b), it is closer to top of the cloud. In nearly every case, z_c falls between the cloud base and cloud top. The large difference for one of the low clouds in Fig. 3a is due to the conversion of T_c to z_c. The cloud is under a sharp inversion that is not resolved by the ECMWF profile. Some of the difference between night and day may be due to the methodologies used. During the daytime, τ is derived using solar reflectance, while at night only the thermal channels are used. Thus, in multilayered cases, the solar channel would overestimate τ for the upper cloud, resulting in an underestimate of the temperature correction and the cloud would be placed lower than expected for the same cloud over a cloud-free background. At night, the optical depth is not affected much by the low clouds because their temperature is close to the clear values. Hence, the derived values would be larger. The day-night difference in the cloud heights is also evident in the VIRS results, but it is smaller by 0.5 km. Despite the differences and a few exceptions, the thin-cloud heights are within the cloud boundaries during all hours.

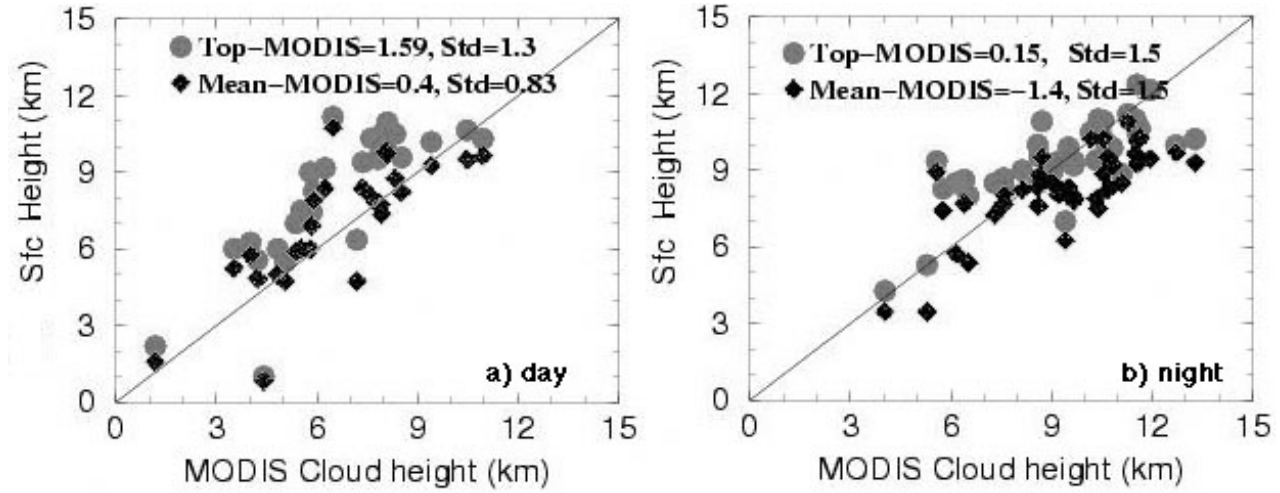

Fig. 3. Comparisons of cloud mean and top heights from surface data and effective heights from MODIS for τ < 5.

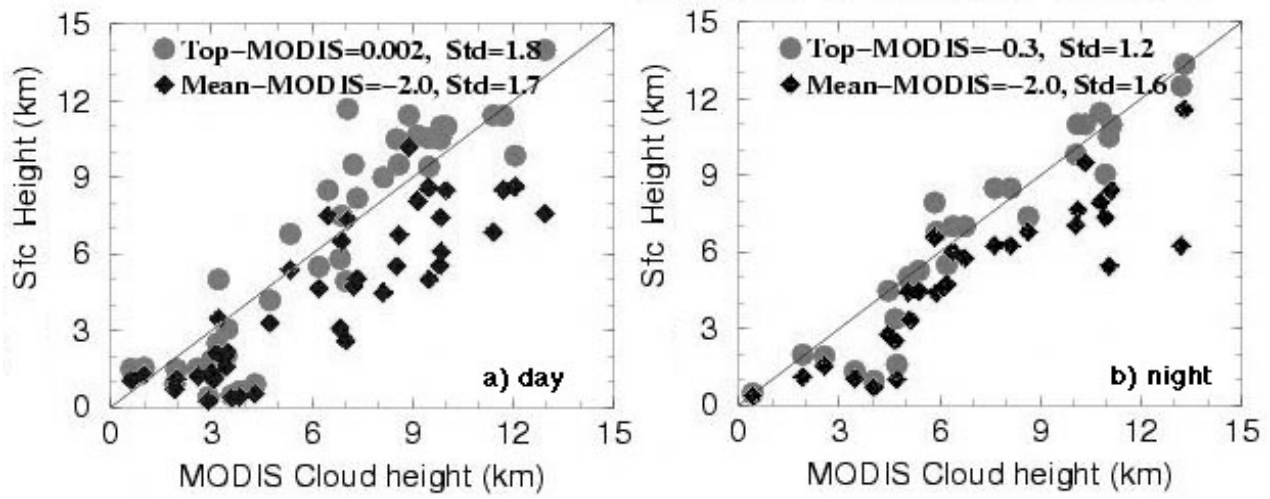

Fig. 4. Same as Fig. 3, except for optically thick clouds ($\tau > 5$).

The optically thick cloud heights are compared in Fig. 4. For high clouds, during the day, z_c falls between the cloud top and center. Most of the optically thick high clouds are several kilometers thick, while the low clouds are typically less than 1-km thick. The inversion effect causes an overestimate of the low-cloud heights from CERES resulting in an average value of z_c that is identical to the top of the clouds during the day and 0.3-km above the cloud tops at night. Removal of the cases affected by the missed inversions results in z_c nearly 1 km below cloud top during the day and nearly the same as cloud top at night. Similar results were found for the VIRS comparisons [16]. The optical depths for stratus clouds over the SGP are compared in Fig. 5 with the CERES daytime retrievals for MODIS (Fig. 5a) and VIRS (Fig. 5b). The values are well correlated in both cases. For the 16 samples in Fig. 5a, the mean MODIS and surface-based optical depths are 31.8 and 29.9, respectively, a 6% difference that is primarily due one outlier. The VIRS mean τ is 20.8, which is 2% smaller than the surface average of 21.3 for the 25 samples. These preliminary comparisons show that the water cloud optical depths are very consistent with surface measurements. Comparisons with single-layer cirrus are underway. In the meantime, it can be concluded that the thin cirrus optical depths are reasonable because they yield temperature corrections that place z_c within the body of the cloud. The consistency between the MODSI and VIR ice and water cloud optical depths shown later further confirm the accuracy of the cloud optical depths derived for CERES.

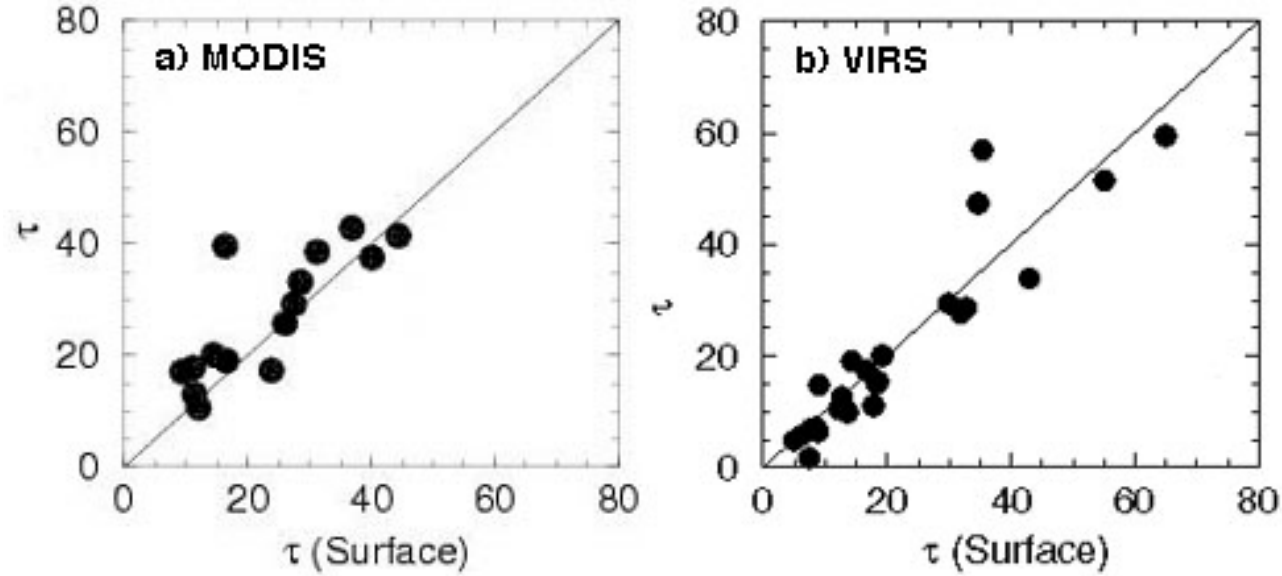

Fig. 5. Comparison of stratus cloud optical depths over the SGP, MODIS (2000-2001) and VIRS (1998).

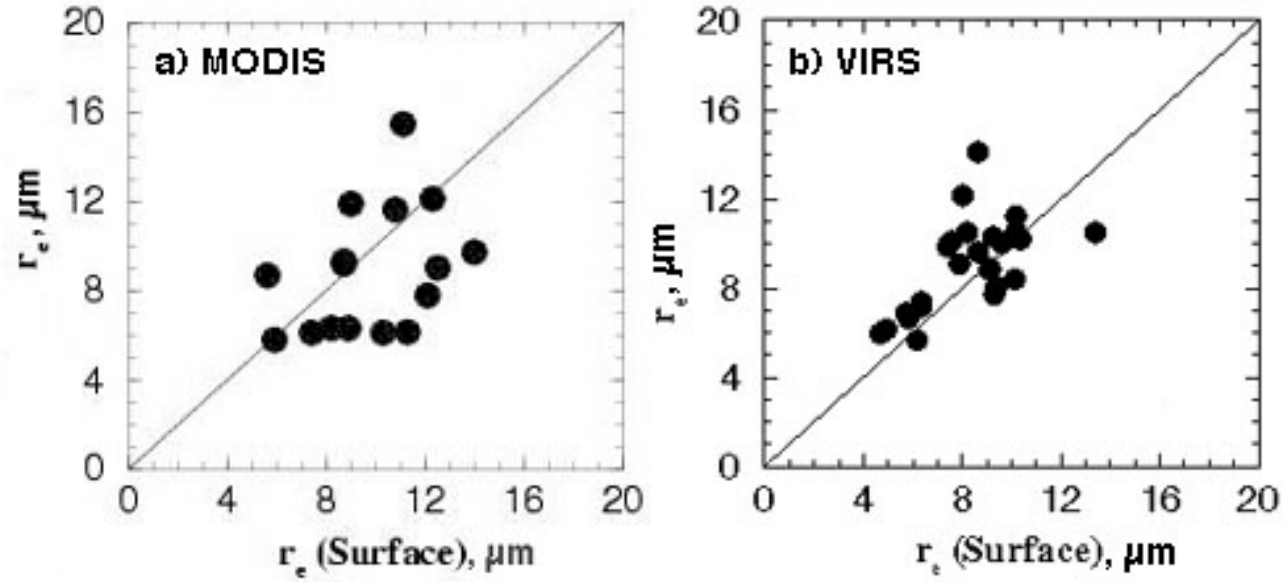

Fig. 6. Same as Fig. 5, except for effective cloud droplet radius.

The stratus cloud effective droplet radii are compared in Fig. 6 for both the MODIS and VIRS data. The mean value of re for MODIS (Fig. 6a) is 8.8 μm, 10% smaller than the surface-derived value. The VIRS mean value of 9.0 μm is 8% less than the surface-based result. The calibration differences between VIRS and MODIS can account for the optical depth differences and ~0.5 μm of the r_e difference. As shown later, the 0.5-μm difference is more typical than would be inferred from Fig. 6. Overall, the CERES-derived mean droplet sizes are within $\pm$ 10% of the surface-based averages. Comparisons of the ice-crystal effective diameters D_e are underway. Earlier comparisons, however, indicate that the CERES retrieval algorithm produces very reasonable values of D_e [20, 21]. Monthly mean liquid WPs (LWP) derived from VIRS for overcast warm (T_c > 273 K) marine areas during 1998 are compared in Fig. 7a with the corresponding values derived from simultaneous collocated TRMM Microwave Imager (TMI) data using a physically based approach [22]. On average, VIRS yields slightly less LWP than TMI. The mean LWP of 176 gm^{-2} derived from MODIS (Fig. 7b) for the stratus cloud cases in Fig. 5a is only 3.5% greater than the SGP average, while VIRS yields a mean value that is 16% greater than the surface. Although more detailed analyses are needed, the initial results show that CERES provides a realistic depiction of the cloud fields.

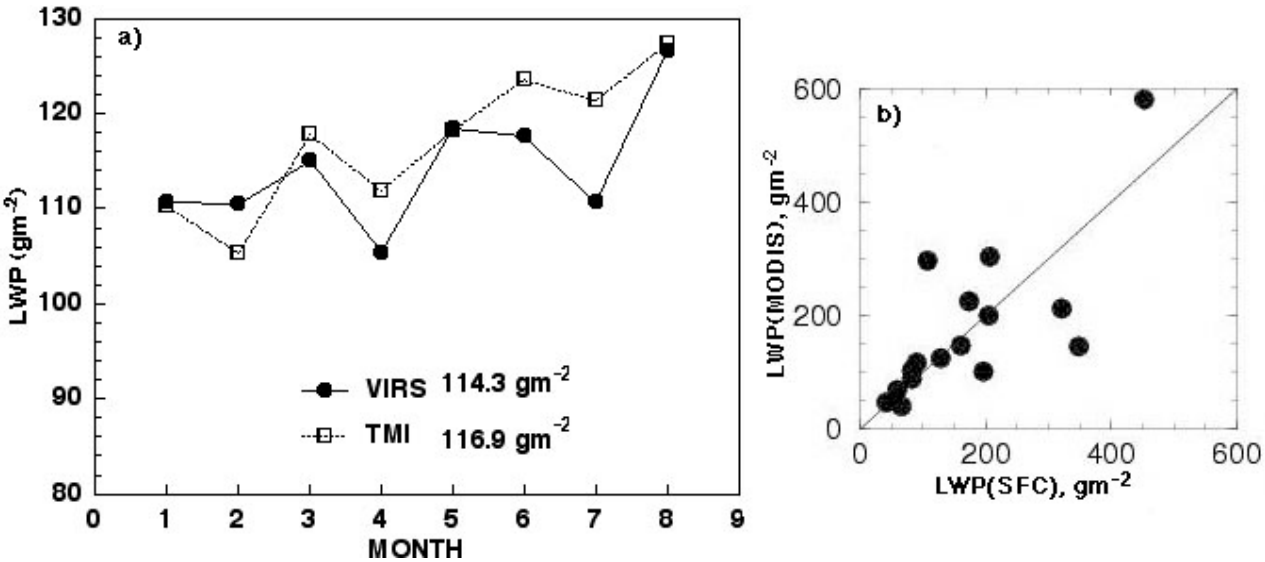

Fig. 7. Comparison of a) monthly LWP for warm clouds over ocean during 1998 and b) for the cases in Fig. 5a.

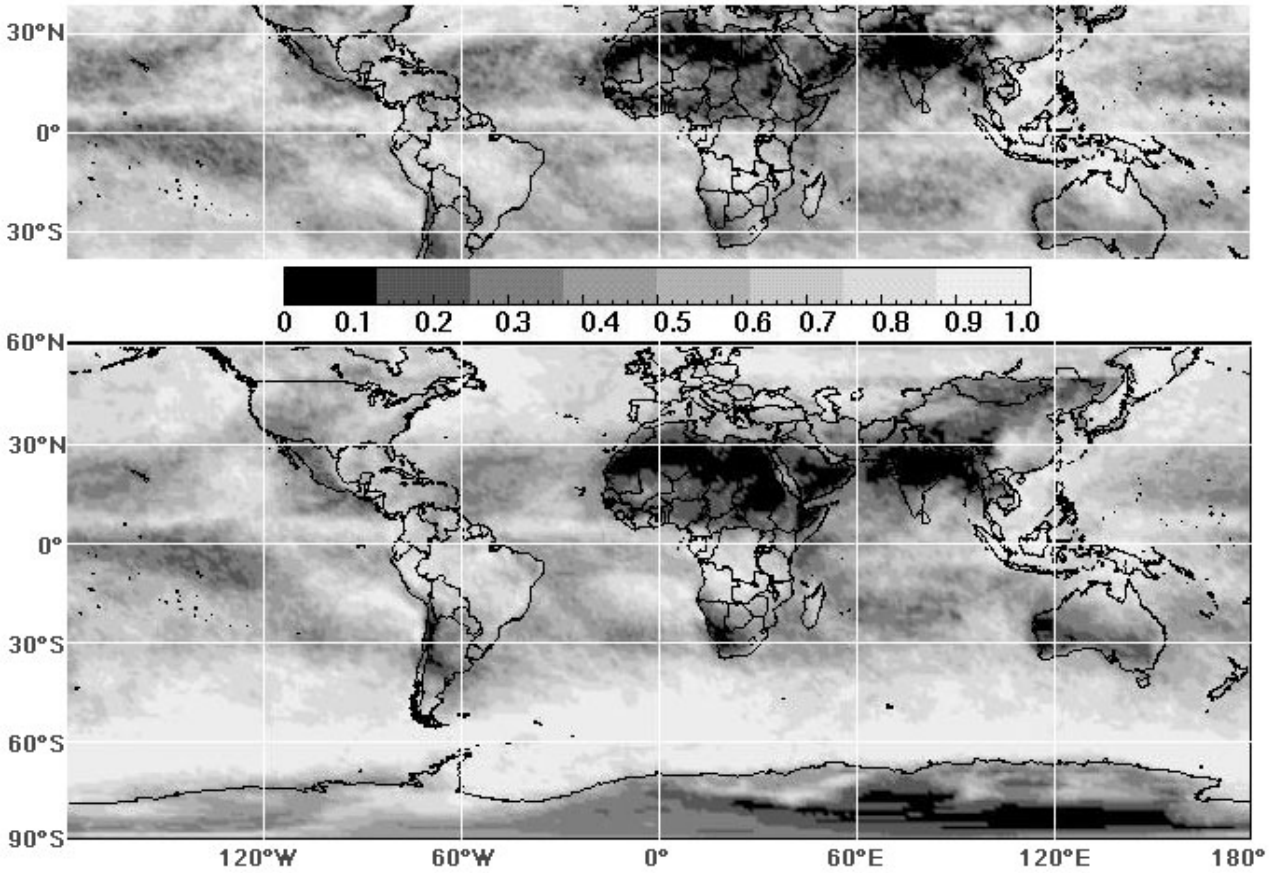

Fig. 8. Monthly mean daytime cloud fraction, December 2000, from VIRS (upper) and MODIS (lower).

CERES analyzes all cloudy pixels. In 3 - 4% of the cloudy cases, cloud properties cannot be retrieved because no match can be found between the modeled and observed radiances. Some of those pixels are reclassified as clear. The remainder are not included in the SSF convolution. Such pixels cannot be processed for a variety of reasons relating to errors in clear-sky radiances, 3-D cloud structure, partially filled pixels, and errors in the parameterizations. Other errors not assessed in the comparisons between the surface and satellite data include those due to overlapped and broken clouds. Thin cirrus over low-level water clouds will often cause an underestimate of the cirrus altitude. If identified as ice (τ of upper-level cloud likely to exceed 2), such pixels will likely yield an underestimate of D_e and τ and an overestimate of WP. If identified as a water cloud, r_e, τ, and WP will be overestimated [23]. Pixels with only partial cloud fraction tend to underestimate τ and overestimate r_e. Variations of each parameter have been quantified as functions of viewing and solar zenith angles and relative azimuth angle [24]. Users of the data should be aware of those dependencies.

4. RESULTS AND CONSISTENCY

The monthly mean daytime cloud amounts for December 2000 are shown in Fig. 8 for both VIRS and MODIS. Although differences on the order of 0.1 occur in some areas, the distribution of cloud amounts is very similar for the two datasets. On average, the MODIS daytime cloud fraction is 0.026 less than the VIRS cloud amount despite the larger viewing zenith angles (VZA) for MODIS ($\leq$ 70°) compared to VIRS ($\leq$ 48°). The VZA effect is probably more than compensated by the higher spatial resolution of the MODIS pixels. Additionally, *Terra* was placed in an orbit to maximize clear skies, while VIRS views nearly all times of day during a month. The sampling and spatial resolution differences probably account for much of the difference in cloud fraction. Figure 9 plots the zonal mean effective cloud heights from the two instruments for December 2000. Over the marine stratus areas, the cloud heights are below 2 km.

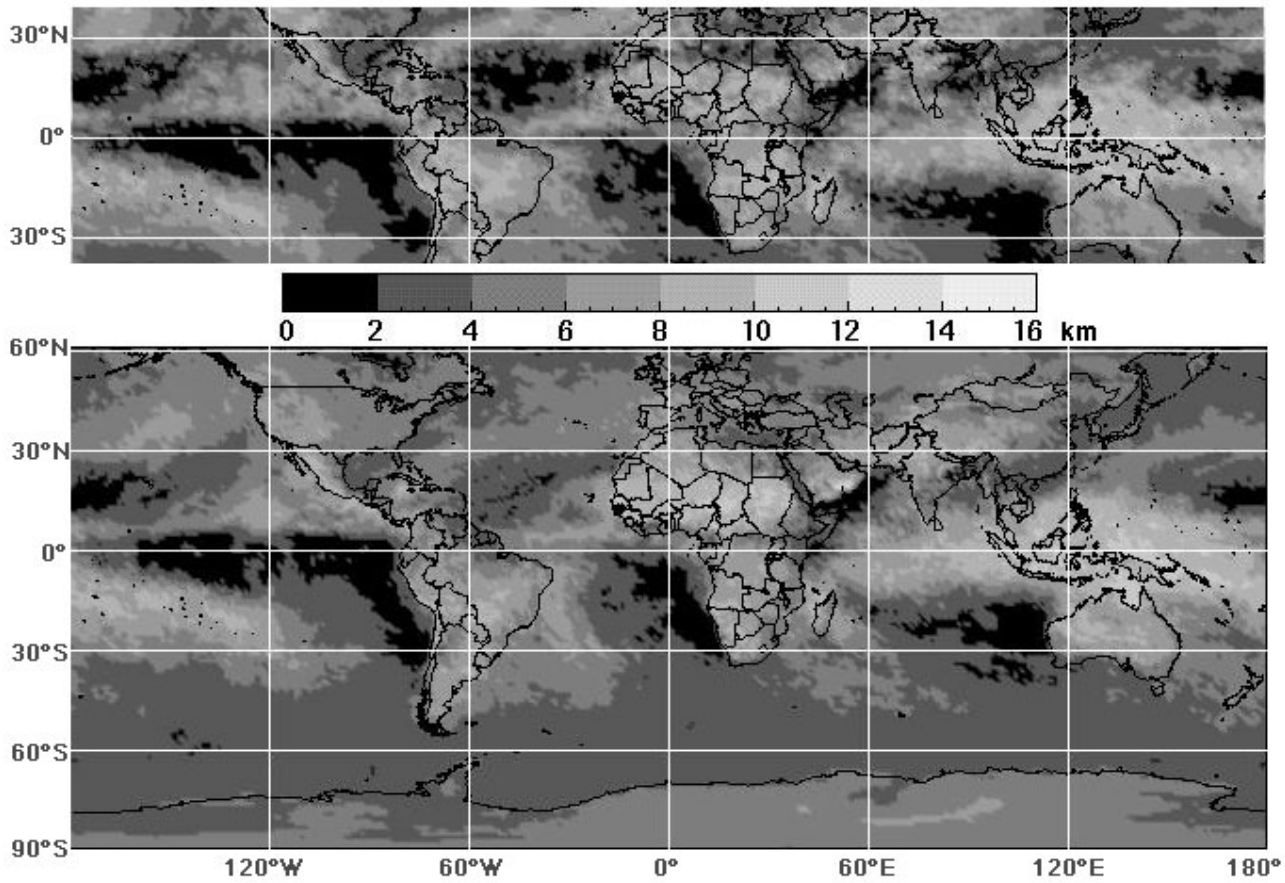

Fig. 9. Same as Fig. 8, except for effective cloud height.

The ECMWF profiles are blended with an artificial boundary-layer temperature profile computed using a -7.1°C/km lapse rate anchored to the sea surface temperature [25]. The ECMWF profile is used above 4 km while a combination of the ECMWF and artificial soundings is used between 2 and 4 km. The artificial sounding is used by itself below 2 km. This approach places the satellite cloud top to within a few hundred meters of the correct altitude in marine stratus environments [26]. The cloud heights in the Southern Hemisphere are very close for both VIRS and MODIS. The regional differences are larger over the Northern Hemisphere most likely due to the VIRS sampling pattern, which observed the Northern Hemisphere fewer times during the day than MODIS. On average, over land, the MODIS ice and water cloud heights are 0.1 ad 0.3-km less than their VIRS counterparts, respectively. Over ocean, the MODIS water clouds are 0.1-km lower, but the ice clouds are 0.2-km higher, than the respective VIRS mean values. The differences are generally consistent with the diurnal cycle in cloud heights.

The mean effective cloud droplet sizes are plotted in Fig. 10 for December 2000. The droplets are smallest over the desert ranging from 5 to 9 μm and in the stratus over China where r_e is between 6 and 8 μm. Over ocean, the smallest droplets are found near the coastal areas water, especially off the west coasts of South America and Africa where r_e is as small as 9 μm in the mean. separately. The VIRS and MODIS patterns are very similar over the Southern Hemisphere and less so in the north. The effective radii from MODIS are, on average, 0.5-μm smaller than their VIRS counterparts, r_e = 13.6 and 10.4 μm over both land and ocean, respectively. The mean values of D_e are plotted in Fig. 11 for both instruments. Again, the patterns are most similar for the Southern Hemisphere. The smallest ice crystals are seen over areas where ice clouds are either infrequent or where only convective blow-off occurs such as near the intertropical convergence zones (ITCZ). Over ocean, D_e from VIRS is 0.5-μm larger than the 52.6 μm average from MODIS. However, over land, the MODIS average of 44.1 μm is 6.2 μm less than the VIRS mean. This difference appears over most regions suggesting, possibly, that the convectively driven diurnal cycle may be responsible. At 1030 LT, most

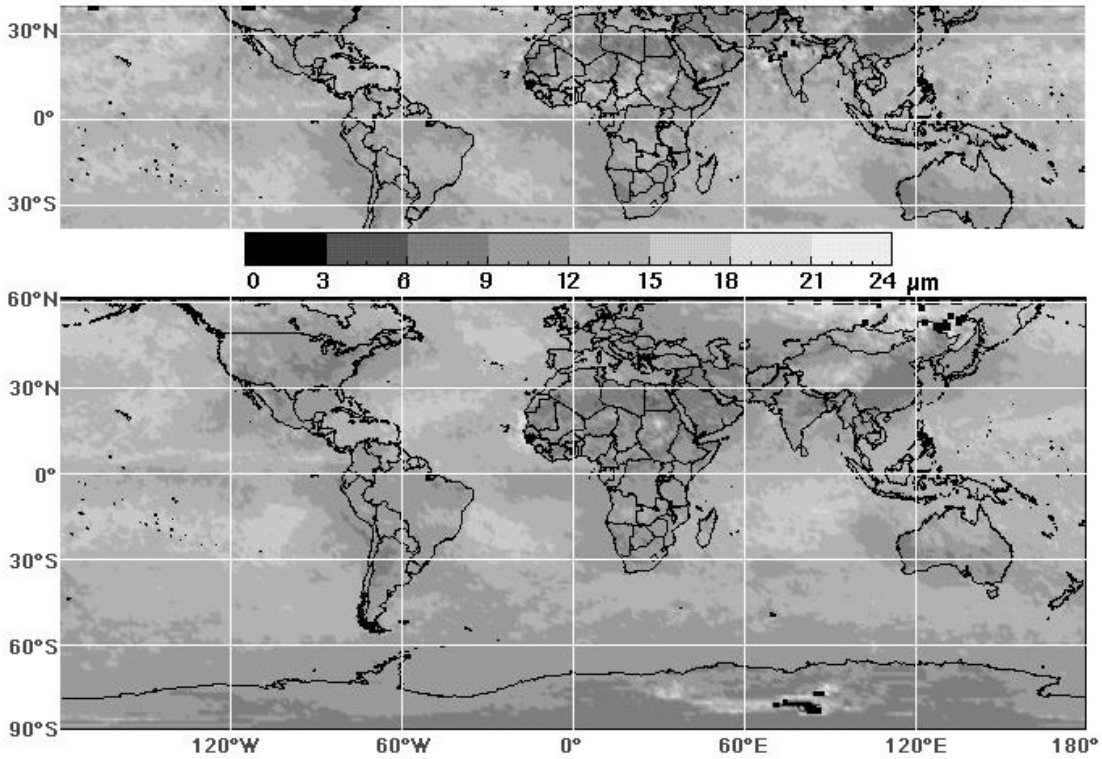

Fig. 10. Mean effective droplet radius for liquid water clouds during December 2000 from VIRS (upper) and MODIS (lower).

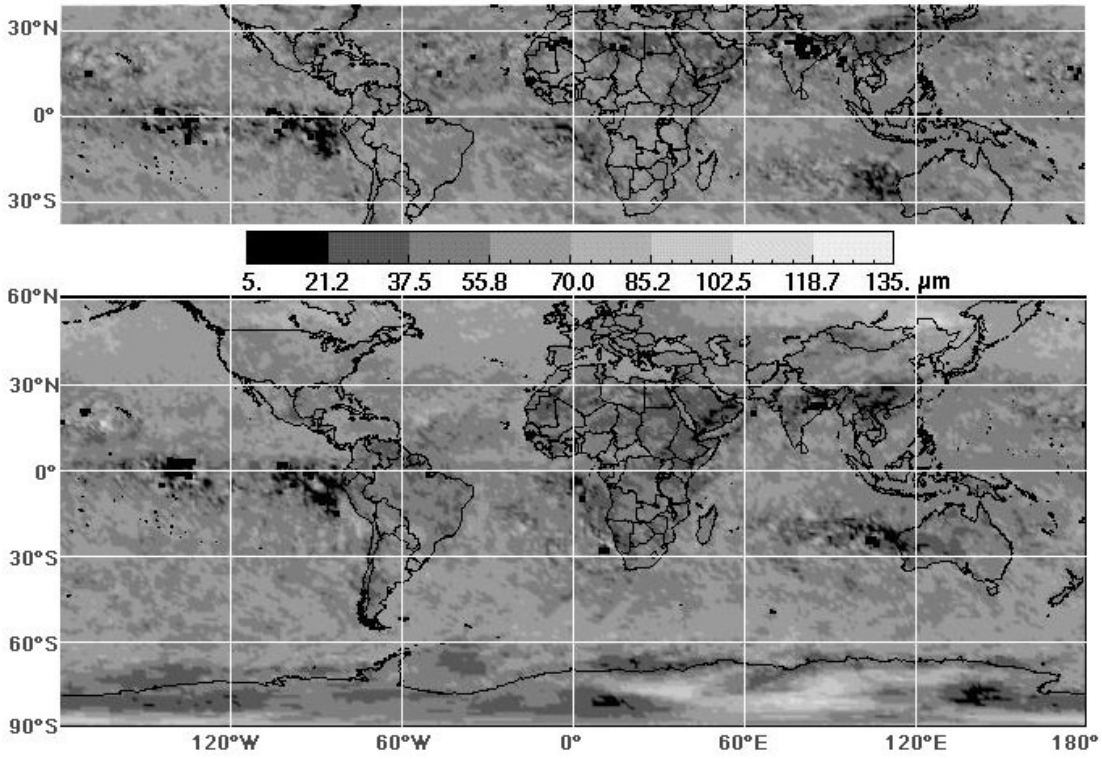

Fig. 11. Mean effective cloud ice crystal diameter during December 2000 from VIRS (upper) and MODIS (lower).

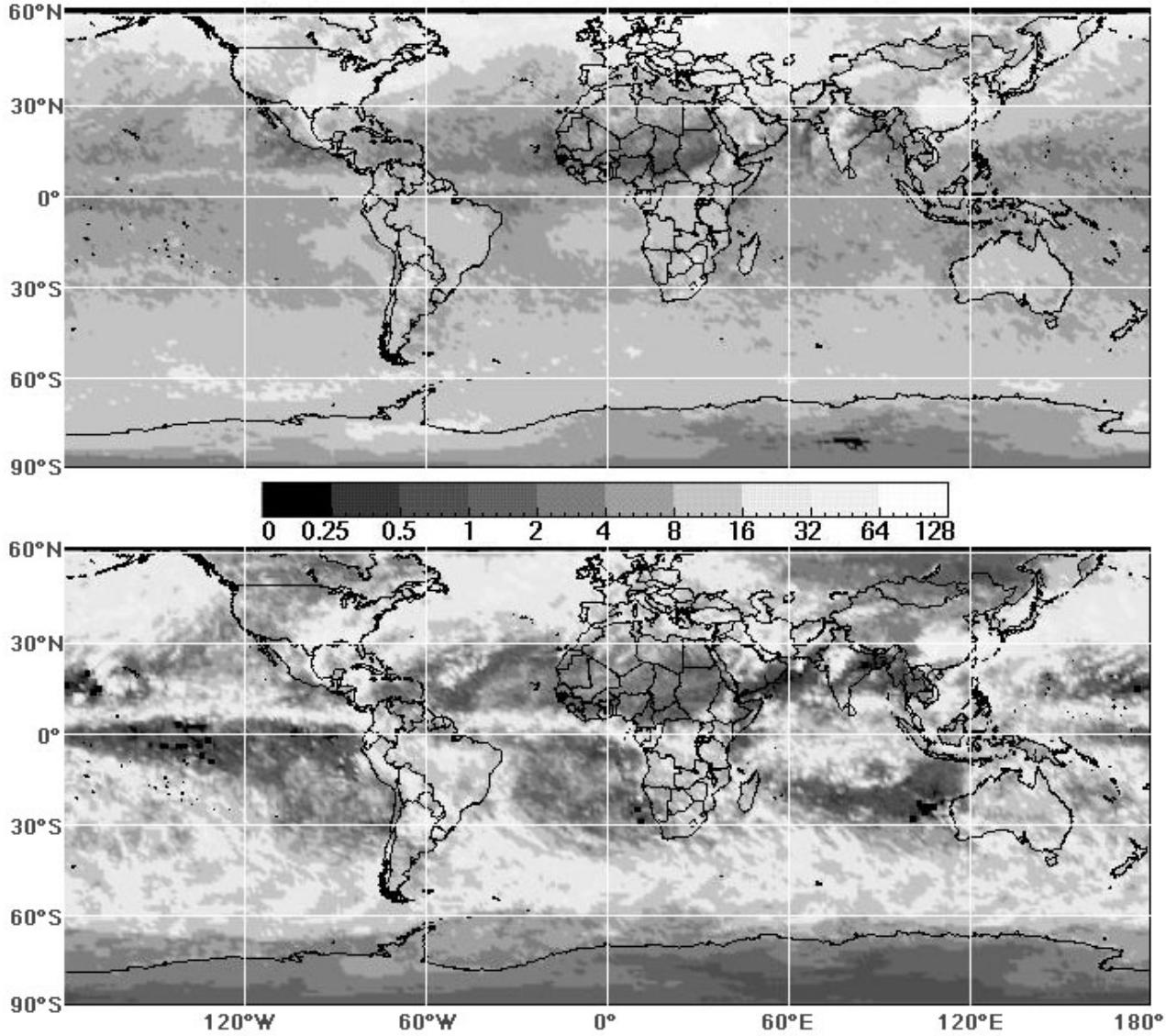

Fig. 12. Mean cloud optical depth from MODIS, December 2000. Liquid water clouds (upper) and ice clouds (lower).

convection has dissipated prior to the daily buildup. Thus, most cirrus clouds that were generated from convective storms would be relatively old and most of the larger crystals would have precipitated out of the clouds. The convective anvils that produce large quantities of large ice crystals are most likely infrequent at 1030 LT over land. This hypothesis is consistent with the optical depth variations. The mean December water and ice cloud optical depths are plotted for MODIS in Fig. 12. The largest water cloud optical depths (OD) are seen over northern storm track near 50°N. Over land, the densest water clouds occur over the eastern USA, China, and Russia. The ice cloud optical depths are greatest over 50°N and 50°S as well as over the ITCZ. On average, the MODIS water cloud ODs over ocean and land, respectively, are 0.3 less than and 0.2 greater than the corresponding VIRS means of 8.0 and 10.9 for December 2000 (not shown). Over ocean, the MODIS ice cloud OD average is 14.4, which is 0.3 smaller than the VIRS mean. Over land, τ(ice) = 19.6 for VIRS, a value that is 46% greater than the MODIS average. This discrepancy is consistent with the diurnal cycle in cloudiness over land, which is usually at a minimum during the mid-to-late morning. The differences in particle sizes and OD translate to small differences in the mean WP except for ice over land. The mean LWP between 37.5°N and 37.5°S from MODIS is 67.6 gm^{-2} for ocean and 78.4 gm^{-2} over land. These values are only 2% and 5% greater than the VIRS averages. The mean ice WP (IWP) from MODIS is 274 gm^{-2} and 211 gm^{-2} over

ocean and land, respectively. Over ocean, IWP(MODIS) is only 1% greater than IWP(VIRS), but it is 30% less than IWP(VIRS). It should be noted that when a liquid water cloud is underneath an ice cloud, the derived WP or OD is for the entire column but is interpreted as all ice or water, not separately for both for a given pixel. Overlapped clouds with τ(ice) < 2 are often interpreted as liquid water clouds while the remainder of overlapped ice-water clouds are almost always retrieved as ice clouds. Thus, IWP is probably overestimated, on average, because precipitating systems usually contain both liquid and solid water. More sophisticated methods are needed to differentiate between the ice and liquid in these mixed phase cloud systems.

5. CONCLUDING REMARKS

A globally robust method as been developed for retrieving cloud properties from high-resolution imager data during day and night. Initial validation efforts show that the CERES-derived cloud products are quite reasonable and are accurate when compared with objective reference data such as ground-based active remote sensing. Much additional study is required to validate and improve some aspects of the retrievals. Nevertheless, the derived products are already being used to study the relationships between cloud properties and the broadband radiance fields [2] and the seasonal and interannual variability in clouds [16]. The results shown here demonstrate some dramatic differences between the CERES cloud properties and those derived from other satellite programs. Additional analysis is required to understand those differences. The consistency between the VIRS Edition 2 and MODIS Edition 1 retrievals is sufficient to examine some of the local time differences in the various properties. They should also be valuable for validating and improving general circulation models and cloud process parameterizations. The CERES cloud and radiation products are available to the general public at http://eosweb.larc.nasa.gov/HBDOCS/langley_web_tool.html.

ACKNOWLEDGMENTS

Thanks to Bing Lin for supplying the matched TMI and VIRS data. This research is sponsored by the NASA Earth Enterprise System through the CERES Program.

REFERENCES

1. Wielicki, B. A., et al., 1998, Clouds and the Earth's Radiant Energy System (CERES): Algorithm overview. *IEEE Trans. Geosci. Remote Sens.*, **36**, 1127-1141.
2. Loeb, N. G. et al., Angular distribution models for top-of-atmosphere radiative flux estimation from the Clouds and the Earth's Radiant Energy System instrument on the Tropical Rainfall Measuring Mission satellite. Part I: Methodology. In press, *J. Appl. Meteorol.*, 2002.
3. Gambheer, A. V., D. R. Doelling, and P. Minnis, Examination of the azimuthal variation of longwave radiance from CERES data. *Proc. 11th AMS Conf. Atmos. Rad.*, Ogden, UT, June 3-7, 2002.
4. Minnis, P., L. Nguyen, D. R. Doelling, D. F. Young, W. F. Miller, and D. P. Kratz, Rapid calibration of operational and research meteorological satellite imagers, Evaluation of research satellite visible channels as references. *J. Atmos. Oceanic Technol.*, **19**, 1233-1249, 2002.
5. Minnis, P., L. Nguyen, D. R. Doelling, D. F. Young, W. F. Miller, and D. P. Kratz, Rapid calibration of operational and research meteorological satellite imagers, Part II: Comparison of infrared channels. *J. Atmos. Oceanic Technol.*, **19**, 1250-1266, 2002.
6. Trepte, Q., Y. Chen, S. Sun-Mack, P. Minnis, D. F. Young, B. A. Baum, and P. W. Heck, Scene identification for the CERES cloud analysis subsystem. *Proc. AMS 10th Conf. Atmos. Rad.*, Madison, WI, June 28 – July 2, 169-172, 1999.
7. Trepte, Q. Z., P. Minnis, and R. F. Arduini, Daytime and nighttime polar cloud and snow identification using MODIS. *Proc. SPIE Conf. Optical Remote Sens. of Atmosphere and Clouds III*, Hangzhou, China, Oct. 23-27, 2002.
8. Sun-Mack, S., Y. Chen, T. D. Murray, P. Minnis, and D. F. Young, Visible clear-sky and near-infrared surface albedos derived from VIRS for CERES. *Proc. AMS 10th Conf. Atmos. Rad.*, Madison, WI, June 28–July 2, 422-425, 1999.

9. Chen, Y., S. Sun-Mack, Q. Z. Trepte, P. Minnis, and D. F. Young, Solar zenith angle variation of clear-sky narrowband albedos derived from VIRS and MODIS. *Proc. 11th AMS Conf. Atmos. Rad.*, Ogden, UT, June 3-7, 152-155, 2002.
10. Chen, Y., S. Sun-Mack, P. Minnis, W. L. Smith, Jr., and D. F. Young, Surface emissivity derived for infrared remote sensing from satellites. *Proc. AMS 11th Conf. Satellite Meteorology and Oceanography.*, Madison, WI, October 15-18, 512-515, 2001.
11. Chen, Y., S. Sun-Mack, Surface spectral emissivity derived from MODIS data. *Proc. SPIE Conf. Optical Remote Sens. of Atmosphere and Clouds III*, Hangzhou, China, Oct. 23-27, 2002.
12. Minnis, P. et al., Cloud Optical Property Retrieval (Subsystem 4.3). In *Clouds and the Earth's Radiant Energy System (CERES) Algorithm Theoretical Basis Document, Volume III: Cloud Analyses and Radiance Inversions (Subsystem 4)*, *NASA RP 1376 Vol. 3*, edited by CERES Science Team, pp. 135-176, 1995.
13. Platnick, S., J. Y. Li, M. D. King, H. Gerber, and P. V. Hobbs, A solar reflectance method for retrieving cloud optical thickness and droplet size over snow and ice surfaces. *J. Geophys. Res.*, **106**, 15185-15199, 2001.
14. Minnis, P., D. P. Garber, D. F. Young, R. F. Arduini and Y. Takano, Parameterizations of reflectance and effective emittance for satellite remote sensing of cloud properties. *J. Atmos. Sci.*, **55**, 3313–3339, 1998.
15. Hahn, C. J., and S. G. Warren, *Extended Edited Synoptic Cloud Reports from Ships and Land Stations Over the Globe, 1952-1996.* NDP026C, Carbon Dioxide Information Analysis Center, Oak Ridge National Laboratory, Oak Ridge, TN, 1999.
16. Minnis, P., et al., Seasonal and diurnal variations of cloud properties derived for CERES from VIRS and MODIS data. *Proc. 11th AMS Conf. Atmos. Rad.*, Ogden, UT, June 3-7, 20-23, 2002.
17. Rossow, W. B. and R. A. Schiffer, Advances in understanding clouds from ISCCP. *Bull Am. Meteor. Soc.*, **80**, 2261-2287, 1999.
18. Dong, X., P. Minnis, G. G. Mace, W. L. Smith, Jr., M. Poellot, R. T. Marchand, and A. D. Rapp, Comparison of stratus cloud properties deduced from surface, GOES, and aircraft data during the March 2000 ARM Cloud IOP. In press, *J. Atmos. Sci.*, 2002.
19. Dong, X., T.P. Ackerman, E.E. Clothiaux, P. Pilewskie, and Y. Han, Microphysical and radiative properties of boundary layer stratiform clouds deduced from ground-based measurements. *J. Geophys. Res.,* **102**, 23 829-23 843, 1997.
20. Young, D. F., P. Minnis, D. Baumgardner, and H. Gerber, Comparison of in situ and satellite-derived cloud properties during SUCCESS. *Geophys. Res. Lett.*, **25**, 1125-1128, 1998.
21. Mace, G. G., T. P. Ackerman, P. Minnis, and D. F. Young, Cirrus layer microphysical properties derived from surface-based millimeter radar and infrared interferometer Data. *J. Geophys. Res.*, **103**, 23,207-23,216, 1998.
22. Lin, B., B. A. Wielicki, P. Minnis, and W. B. Rossow, Estimation of water cloud properties from satellite microwave and optical measurements in oceanic environments. I: Microwave brightness temperature simulations. *J. Geophys. Res.*, **103**, 3873-3886, 1998.
23. Kawamoto, K., P. Minnis, W. L. Smith, Jr., and A. D. Rapp, Detecting multilayer clouds using satellite solar and IR channels. *Proc. 11th AMS Conf. Cloud Physics.*, Ogden, UT, June 3-7, CD-ROM, JP1.18, 2002.
24. Heck, P. W., P. Minnis, D. F. Young, and S. Sun-Mack, Angular variations of cloud properties from VIRS and MODIS data. *Proc. 11th AMS Conf. Atmos. Rad.*, Ogden, UT, June 3-7, 148-151, 2002.
25. Minnis, P., P. W. Heck, D. F. Young, C. W. Fairall, and J. B. Snider, Stratocumulus cloud properties derived from simultaneous satellite and island-based instrumentation during FIRE, *J. Appl. Meteor.*, **31**, 317-339, 1992.
26. Garreaud, R. D., J. Rutllant, J. Quintana, J. Carrasco, and P. Minnis, CIMAR-5: A snapshot of the lower troposphere over the subtropical southeast Pacific. *Bull. Amer. Meteor. Soc*., **92**, 2193-2208, 2001.